International Journal of Innovative Technology and Exploring Engineering (IJITEE)
ISSN: 2278-3075 (Online), Volume-9 Issue-2, December 2019

Machining Performance of Aluminium 7075 Composite: A Grey Based Taguchi Concept

Diptikanta Das, Bharat Chandra Routara, Basanta Kumar Nanda, Soham Chakraborty

Abstract*: Irregular particulates of Silicon carbide (SiC_p) augmented aluminium 7075 metal matrix composite (MMC) was processed by vortex route of stir casting. Homogeneous dispersion of the reinforcement was verified by metallurgical microscope. Machining performance of the synthesized MMC was investigated during turning, considering surface roughness, cutting temperature, tool flank wear and material removal rate as performance criteria. The chips formed during the turning trials were also analyzed. The machining quality targets were optimized simultaneously through grey relational analysis (GRA) based Taguchi method, which resulted that the optimal combination of parametric levels was 154 $m.min^{-1}$, 0.04 $mm.rev^{-1}$and 0.1 mm of cutting speed (V), feed (f) and cutting depth (d), respectively. Mathematical models were then generated for the individual responses using response surface method, followed by verification of their adequacy.

Keywords: Composite, Grey relational analysis, Response surface model, Turning

I. INTRODUCTION

Superior mechanical properties, high corrosion resistances and low density of Al based MMCs make them potential for application in aerospace and automotive industries [1-4]. However, consistent dispersion of reinforced particles [5] and machining [6] are some of the major challenges for these materials. Though different processes have been investigated to synthesize the MMCs, liquid processing method is widely followed, because of their economical mass production in this process [7]. Presence of hard ceramic particles causes difficulty in machining, leading to high tool wear rate and deteriorated surface quality [8-11].

Lin et al. [12], while machining SiC_p reinforced aluminium 359 MMC using Poly Crystalline Diamond (PCD) tools reported the deterioration of surface finish at higher feed, but there was not significant change with speed of cutting.

Revised Manuscript Received on December 30, 2019.
***** Correspondence Author
Diptikanta Das, School of Mechanical Engineering, KIIT Deemed to be University, Bhubaneswar, India. Email: diptikantadas115@gmail.com
Bharat Chandra Routara*, School of Mechanical Engineering, KIIT Deemed to be University, Bhubaneswar, India. Email: bcroutray@gmail.com
Basanta Kumar Nanda, School of Mechanical Engineering, KIIT Deemed to be University, Bhubaneswar, India. Email: bnandafme@kiit.ac.in
Soham Chakraborty, School of Mechanical Engineering, KIIT Deemed to be University, Bhubaneswar, India. Email: sohm13@gmail.com

Moreover, with increasing the speed of cut or feed rate, the flank surface worn out quicker, which was as a result of elevated tool tip temperature at greater speed and feed levels. Ciftci et al. [13] reported lower surface imperfections and more tool flank wear while cutting aluminium 2014/SiC_p MMCs in dry machining condition using un-coat WC tools in comparison to TiC/Al_2O_3/TiCN coated WC inserts; and increase of tool wear was reported on increasing either of cutting speed, reinforcement particlate size or reinforcement concentration in the MMCs. Ding et al. [14], during cutting Al/SiC_p MMCs using Poly Crystalline Boron Nitride (PCBN) and PCD inserts in both dry and wet environment, observed better machining performance with the PCD inserts. Surface roughness, abrasion on the tool flank face and groove wear increased when coolant was used during machining. More rate of material removal along with improved surface finish on increasing the cutting speed was noticed by Venkatesh et al. [15], while cutting aluminium 356/SiC_p MMC with PCD tool. Built up edge (BUE) was observed on rake surface; and hard ceramic reinforcements present in the matrix alloy caused abrasion leading to tool wear. Minimum value of mean surface roughness was noticed during cutting LM6/SiC_p MMC with PCD tools at the lowest level of reinforcement content (7.5 wt.%), minimum cutting depth (0.5 mm) and maximum cutting velocity (90 $m.min^{-1}$) [16]. Decreased roughness of AA 2124SiC_p MMC was reported by Schubert and Nestler [11], during turning the material using diamond tipped tools with wiper geometry. Surface finish of the material was affected by width of flank wear in the cutting tool. Improved quality of surface and accelerated tool flank wear were reported by Sahoo et al. [17] at higher cutting speed, during turning SiC_p impregnated Al MMC with multi TiN-layer coated WC inserts. Also, with the increase of feed, the surface quality deteriorated and flank wear increased. From the results of Analysis of variance during machining Al/SiC_p MMC, Sahoo and Pradhan [18] reported speed of cutting was most influential for surface roughness, next to feed; however, for tool flank wear feed was most influential, next to cutting speed. Moreover, for both the responses depth of cut was insignificant. During dry turning the chemically synthesized Al/TiC MMCs using uncoated ceramic tools, Kumar et al. [6] reported higher surface roughness values at low speed of cutting, high rate of feed and large cutting depth. Formation of less amount of BUE was the basic reason for good quality of surface at greater levels of cutting speed.

Mishra et al. [19], during straight turning the SiC_p impregnated aluminium 7075 MMCs by uncoated WC tools in both dry and spray cooled conditions, noticed lower values of surface roughness and tool temperature in spray cooled condition than those in dry condition for the identical levels of speed, feed and cutting depth. Bhuyan and Routara [3] optimized the machining parameters through VIKOR followed by entropy weight method while electro discharge machining (EDM) Al/18 wt.% SiC_p MMCs, and reported that 116 µsec pulse on time, 20 Amp pulse current and 0.836 Kg/cm^2 flushing pressure were the optimized cutting factors for the multi performance machining criteria (rate of material removal, rate of tool wear, radial overcut and average roughness of machined surfaces). During turning the thermally-treated aluminium MMCs with titanium nitride coated WC cutting tools in spray cooled environment, Das et al. [20] reported that 40 $m.min^{-1}$, 0.05 $mm.rev^{-1}$ and 0.2 mm of V, *f* and *d* were the optimal factor setting for various response targets, where the optimization problem was solved through WPCA (weighted principal component analysis) based on Taguchi method.

Above discussion reveals that machining performance of Al/SiC_p MMCs was influenced by the types of matrix and reinforcement used, particle size and their % of reinforcement, levels of machining parameters, machining environment etc. Very few literature is available on investigation of influence of turning parameters on cutting temperature and material removal rate of Al 7075 MMCs. Accordingly, in this paper the machining performance of aluminium 7075/SiC_p MMC is investigated with respect to arithmetic average of surface roughness (*Ra*), cutting tool surface temperature (*T*), tool flank wear (*VBc*), material removal rate (*M*) and chip forms using the low cost uncoated carbide inserts in dry environment. Moreover, GRA and Taguchi method are used for simultaneous optimization of the quality targets under consideration. Finally, mathematical models are generated for the quality targets using response surface method.

II. MATERIALS AND METHODS

Discontinuous SiC_p (20 wt.% and average particle size of 30.65 µm) incorporated aluminium 7075 matrix composites were synthesized following vortex stir casting route. Table I presents elemental composition the matrix alloy. During the MMC synthesis, sliced Al ingots were melted and superheated to 820 ± 10^0C in a three phase electrical furnace. Vortex was generated on the liquid alloy surface during stirring it mechanically at a speed of around 160 rpm. Preheated (900^0C) SiC particulates were entered into the generated vortex manually at around 10 g/min. After completing the SiC addition, the stirring process was pursued for about 10 min at an increased speed of 230 rpm. Position of the stirrer was about one-third height of the composite slurry from its bottom. Some degasser (hexachloroethane) was then added to the slurry to restrict the H_2 contamination. At the end, the degassed composite slurry was filled into a mould at 800^0C, made of alloy steel. Fig. 1 presents the synthesized MMC sample. Dispersion pattern of the reinforced particles was observed by an inverted microscope (Lieca-DMI3000 M) and the micrograph (Fig. 2) depicts consistent dispersion of the SiCp in the aluminium alloy. The composite workpiece deployed for the turning trials was of 50 mm diameter and 110 mm length. But machining was carried out for 80 mm length. Hardness of the workpiece was 70 HRB.

The MMC specimen was turned in dry condition using HMT-NH 22 precision lathe. WIDIA make uncoated WC cutting tools (SNMG 120408) mounted rigidly to PSSNR 2525M 12 tool holder were utilized for metal cutting during turning. The workpiece was securely backed up by tailstock during turning. Cutting speed (*V*), feed (*f*) and depth of cut (*d*) were the variables (machining parameters) during the turning trials, each assigned to four levels (Table II). Moreover, the turning trials followed Taguchi L_{16} DOE (Table III).

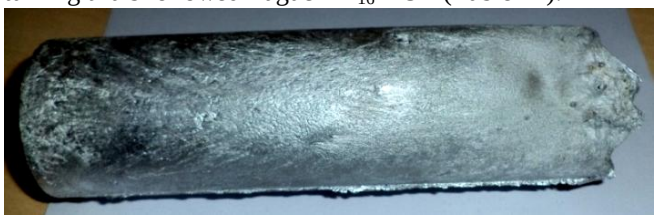

Fig. 1. As-synthesized MMC sample.

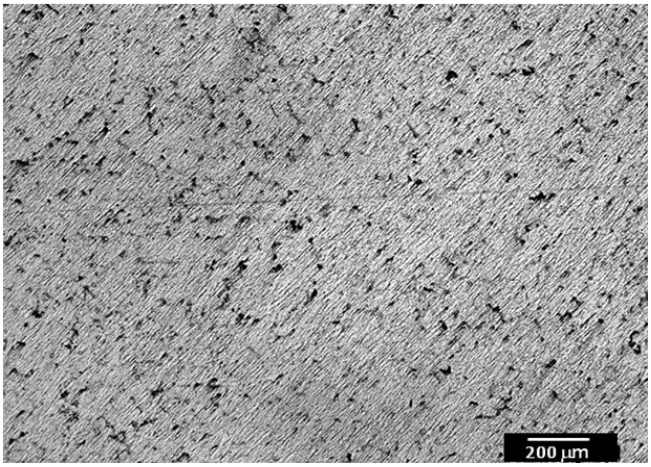

Fig. 2. Optical micrograph of the MMC sample.

Table I: Results of chemical composition test

Constituents	Wt.%	Constituents	Wt.%
Zn	5.60	Mn	0.137
Mg	2.46	Ti	0.044
Cu	1.39	Cr	0.198
Si	0.143	Al	88.9
Fe	3.313	Others	Rest

Table II: Parameters of machining with their levels

Machining parameter	Levels			
	1	2	3	4
Cutting speed (V), $m.min^{-1}$	40	81	98	154
Feed (f), $mm.rev^{-1}$	0.04	0.08	0.12	0.16
Depth of cut (d), mm	0.1	0.3	0.5	0.7

Fluke-Ti32 infrared (IR) thermal imager was employed for measurement of *T* during turning and it was positioned at about 200 mm from the work-tool interface. Fig. 3 presents the experimental setup while conducting turning trials of the MMC.

After each turning trial, *Ra* was evaluated by Taylor Hobson surface roughness tester of model Surtronic 25 (Fig. 4). *VBc* was measured and images of worn cutting edges were captured using Olympus-STM 6 optical microscope (Fig. 5) installed with Stream Basic analysis software. As the cutting depth was smaller than radius of tool nose (0.8 mm), *VBc* was measured at the nose corner only. All the measurements followed three-times average method. *M* was calculated using the formula mentioned in Eq. (1) [19].

$$M(mm^3/\min) = \frac{\pi}{4}(D_1^2 - D_2^2).f.N \quad (1)$$

Here D_1 and D_2 symbolize diameters of composite sample prior to and after turning (mm), and *N* symbolizes spindle speed of the lathe (rpm).

Fig. 3. Turning setup of the MMC.

Fig. 4. Surface roughness measurement.

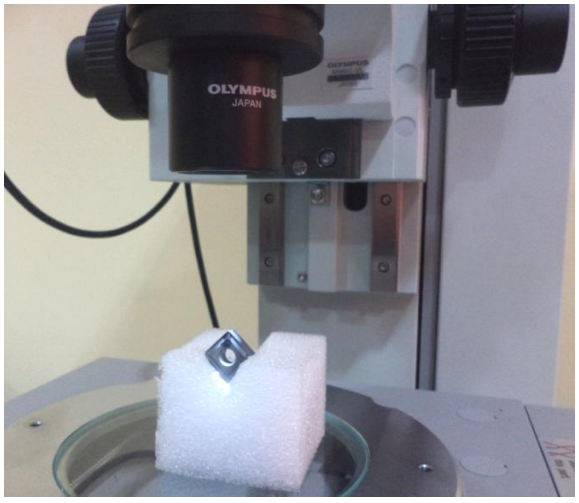

Fig. 5. Measurement of tool flank wear.

III. RESULTS AND DISCUSSION

A. Effect of machining process parameters

Table III presents results of experimentation for *Ra*, *T*, *VBc* and *M* while turning the MMC in dry condition.

Maximum value of *Ra* (3.44 µm) was observed for trial 4, i.e. for minimum cutting speed, maximum feed and at depth of cut 0.7 mm. At the same cutting depth while turning with maximum cutting speed level and minimum feed (trial no. 13), minimum value of *Ra* (1.25 µm) was observed. From the above observation, it is evident that *Ra* is highly influenced by cutting speed; and high speed machining produces surfaces of better quality. Moreover, while machining the MMC at constant cutting speed at increased feeds and reduced depth of cuts (trial nos. 13-16), the *Ra* value increased consistently. Main effects plot for Ra is shown in Fig. 6 (a), which reveals that the mean *Ra* value decreased with increase of speed of cutting; but it increased parallel with feed and cutting depth. BUE formation and more tool-work contact area at low cutting speed may be the reason behind higher *Ra* values. During high speed machining, the BUE formation and the tool-work contact area reduces, thus by improving the surface quality. On increasing feed of machining, more thrust force is induced which leads to vibration and deteriorated surface quality. Similarly, increasing depth of cut during machining the MMC, more amount of reinforcement particles are fractured leading to void formation and increase in *Ra* [6]. Optical micrographs of machined surfaces of the MMC sample are shown in Fig. 7 (a-d), which reveal particle fracture, particle pull out and formation voids.

Minimum value of *T* (38.7^0C) was observed for trial no. 1, i.e. while turning the MMC at the minimum parametric levels. It was maximum (84.12^0C) at *V*, *f* and *d* of 154 m.min^{-1}, 0.04 mm.rev^{-1} and 0.7 mm, taken in sequence (trial no. 13). Further, from the trials 13-16, it was observed that even turning at constant *V*, *T* reduced with increasing *f* and reducing *d*. It clearly explained that depth of cut was more influential than feed for *T*. However, increase in any of the machining parameters caused increase in mean *T* (Fig. 6 b). At higher levels of these parameters more heat is generated at the machining zone due to increased friction, which causes increase in *T*. Infrared thermal images of some trials are exhibited in Fig. 8 (a-d) as exemplar.

Experimental outcomes for VBc (Table III) divulge that the wear on flank surface was least (0.101 mm) at the minimum levels of machining parameters, i.e. at 40 m.min^{-1}, 0.04 mm.rev^{-1}and 0.1 mm of *V*, *f* and *d*, respectively (trial no. 1); and highest (0.303 mm) at 154 m.min^{-1}, 0.16 mm.rev^{-1} and 0.1 mm of *V*, *f* and *d*, respectively (trial no. 16). In all the trials (except trial no. 16) the *VBc* was bellow 0.3 mm (limiting criterion as per ISO 3685:1993), which was because of stable BUE formation on the tool tip that protected its rapid wear. At the combination of highest levels of *V* and *f* (trial no. 16) the VBc just crossed 0.3 mm. Main effects plot of *VBc* (Fig. 6 c) depicts that the mean *VBc* increased on increasing *V* or *f*; but *d* was insignificant. At higher parametric levels friction between flank face and reinforced abrasives increases, which causes an increased *VBc*. Flank wear image of some trials are portrayed in Fig. 9 (a-d). Though abrasion was the predominant mechanism of flank wear, adhesion was also reported on the rake surface at low cutting speeds causing BUE formation.

At the higher speeds of cutting, deep scratches are clearly visible on the flank surface (Figs. 9 c and d), which are due to abrasion with hard reinforcements.

Least value of *M* (90.34 mm^3/min) was noticed at parametric settings of 40 $m.min^{-1}$, 0.04 $mm.rev^{-1}$ and 0.1 mm; however, that increased to 6105.3 mm^3/min while turning the MMC at 154 $m.min^{-1}$, 0.08 $mm.rev^{-1}$ and 0.5 mm of *V*, *f* and *d*, taken in sequence. Main effects plot of *M* (Fig. 6 d) depicts that *M* increases on increasing *V*, *f* or *d*, i.e. high speed cutting of the composite at higher values of *f* and *d* results more material removal, leading to increased productivity.

Table III: Results of turning experiments

Trial No.	V	f	d	Ra (μm)	T (^{0}C)	VBc (mm)	M (mm^3/min)
1	40	0.04	0.1	1.37	38.77	0.101	90.34
2	40	0.08	0.3	1.83	54.83	0.143	549.55
3	40	0.12	0.5	2.96	62.38	0.189	1411.57
4	40	0.16	0.7	3.44	70.83	0.232	2740.46
5	81	0.04	0.3	1.54	55.53	0.133	666.70
6	81	0.08	0.1	1.94	49.53	0.170	449.99
7	81	0.12	0.7	2.38	80.33	0.203	4841.01
8	81	0.16	0.5	2.62	80.43	0.244	4776.33
9	98	0.04	0.5	1.29	67.37	0.149	3597.22
10	98	0.08	0.7	1.83	79.90	0.189	4623.14
11	98	0.12	0.1	1.86	61.10	0.236	1012.23
12	98	0.16	0.3	2.35	72.87	0.277	4092.05
13	154	0.04	0.7	1.25	84.12	0.167	4146.01
14	154	0.08	0.5	1.48	78.60	0.204	6105.30
15	154	0.12	0.3	2.01	67.00	0.255	5604.23
16	154	0.16	0.1	2.11	63.12	0.303	2515.09

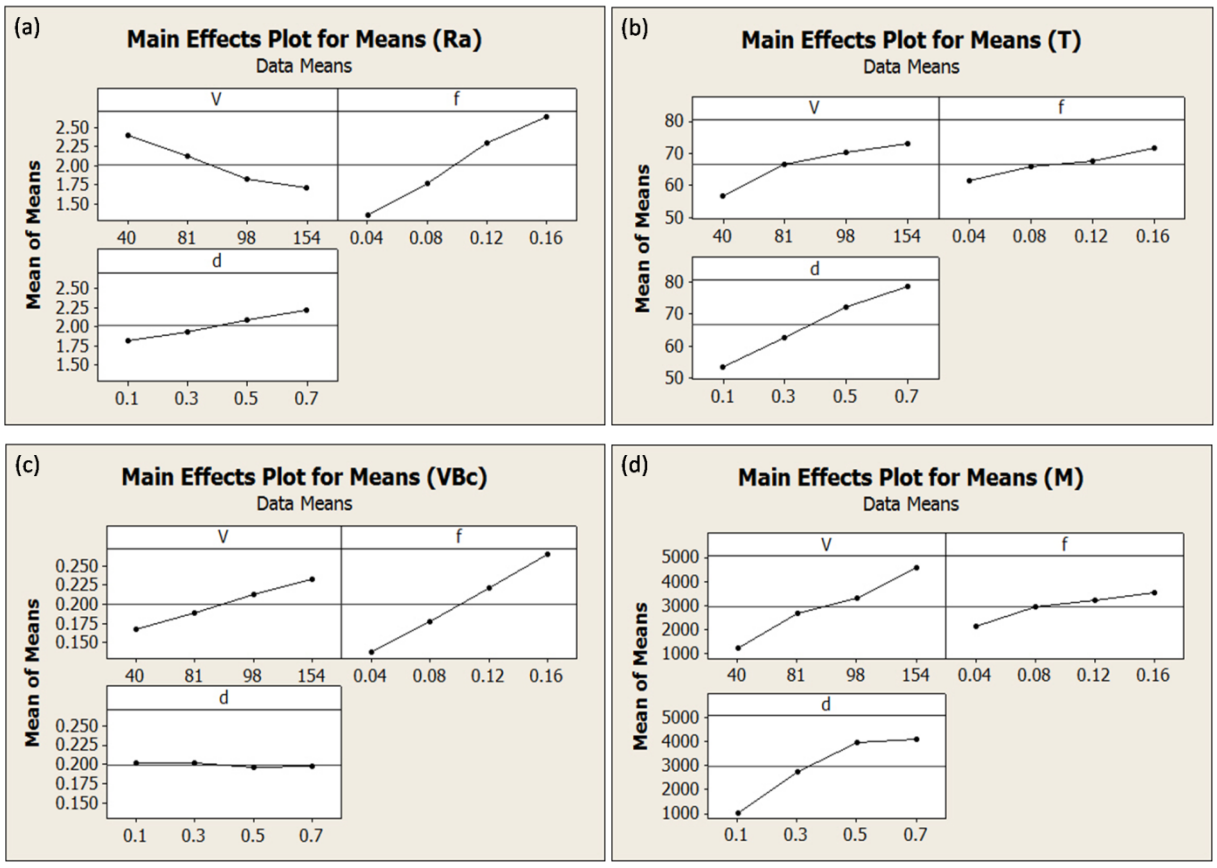

Fig. 6. Main effects plots for the means of (a) *Ra*; (b) *T*; (c) *VBc* and (d) *M*.

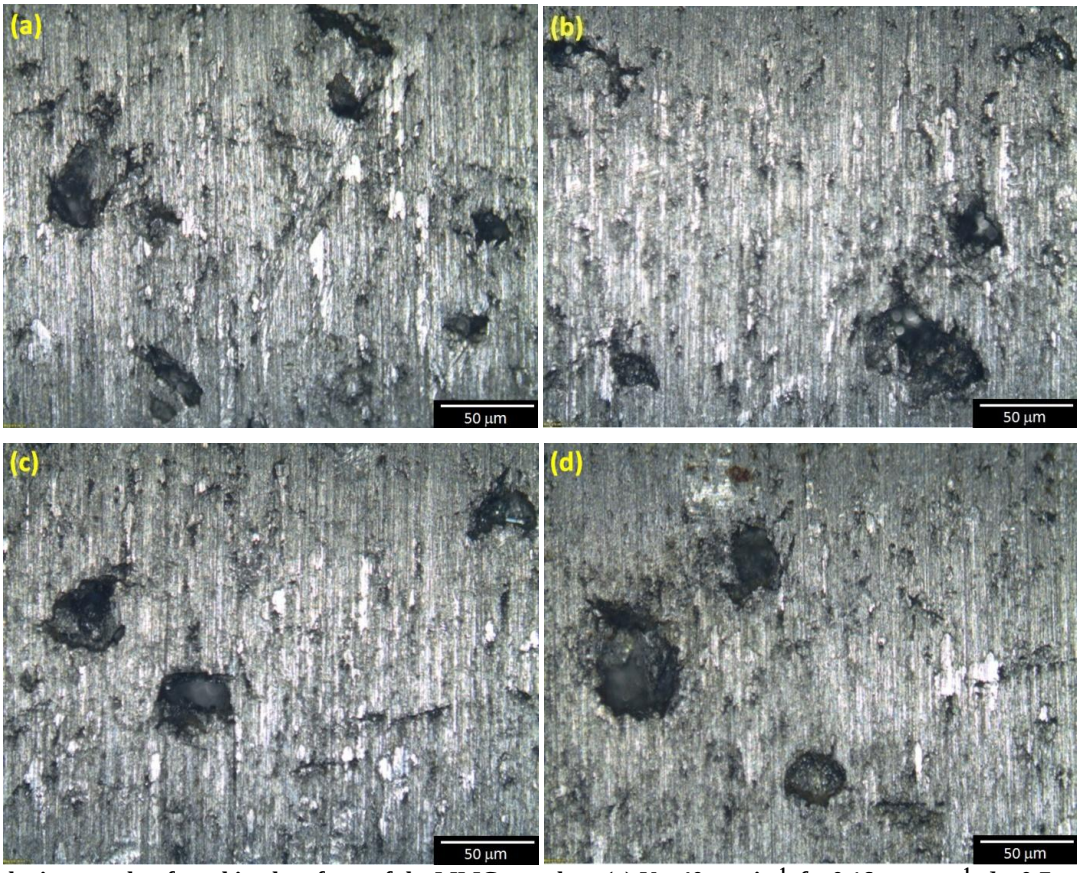

Fig. 7. Optical micrographs of machined surfaces of the MMC sample at (a) V = 40 m.min^{-1}, f = 0.16 mm.rev^{-1}, d = 0.7 mm; (b) V = 81 m.min^{-1}, f = 0.16 mm.rev^{-1}, d = 0.5; (c) V = 98 m.min^{-1}, f = 0.16 mm.rev^{-1}, d = 0.3 and (d) V = 154 m.min^{-1}, f = 0.16 mm.rev^{-1}, d = 0.1.

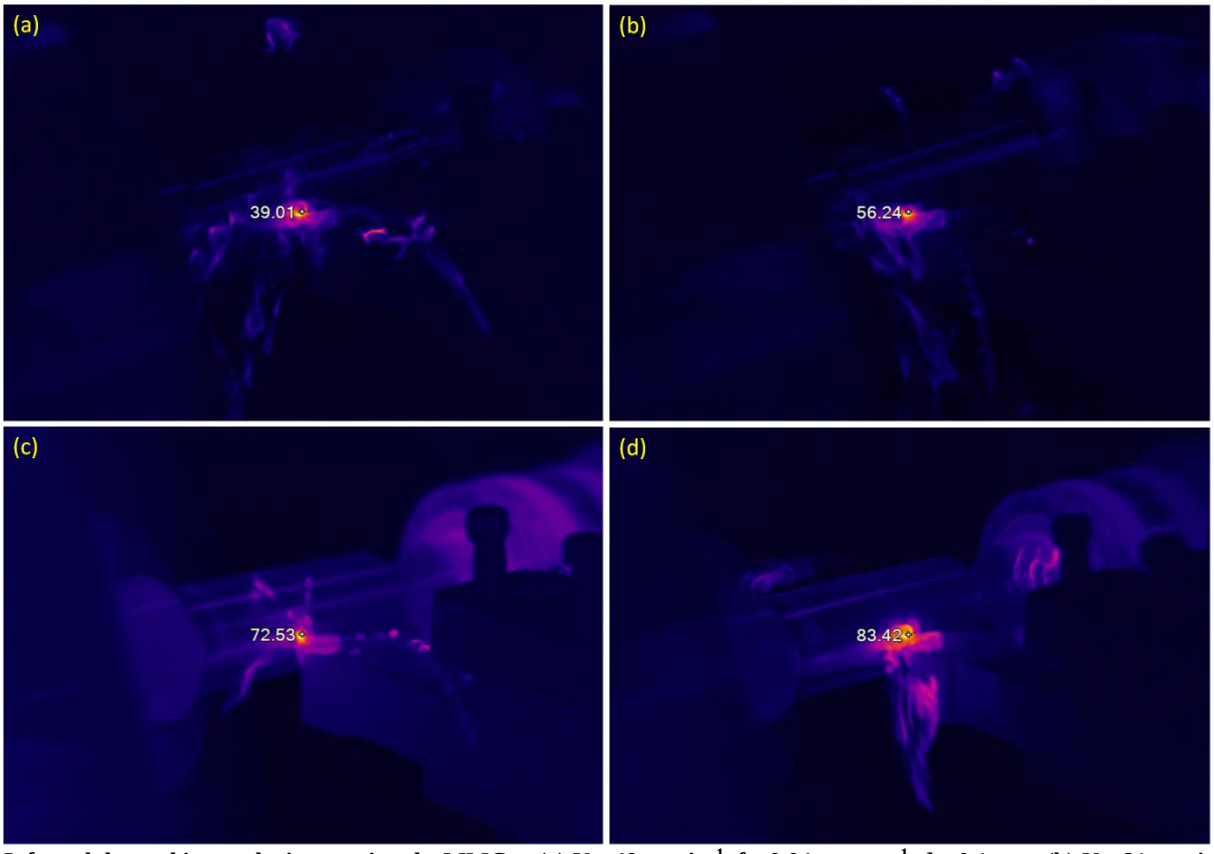

Fig. 8. Infrared thermal image during turning the MMC at (a) V = 40 m.min-^{1}, f = 0.04 mm.rev^{-1}, d = 0.1 mm; (b) V = 81 m.min-^{1}, f = 0.04 mm.rev^{-1}, d = 0.3 mm; (c) V = 98 m.min-^{1}, f = 0.16 mm.rev^{-1}, d = 0.3 mm; and (d) V = 154 m.min-^{1}, f = 0.04 mm.rev^{-1}, d = 0.7 mm.

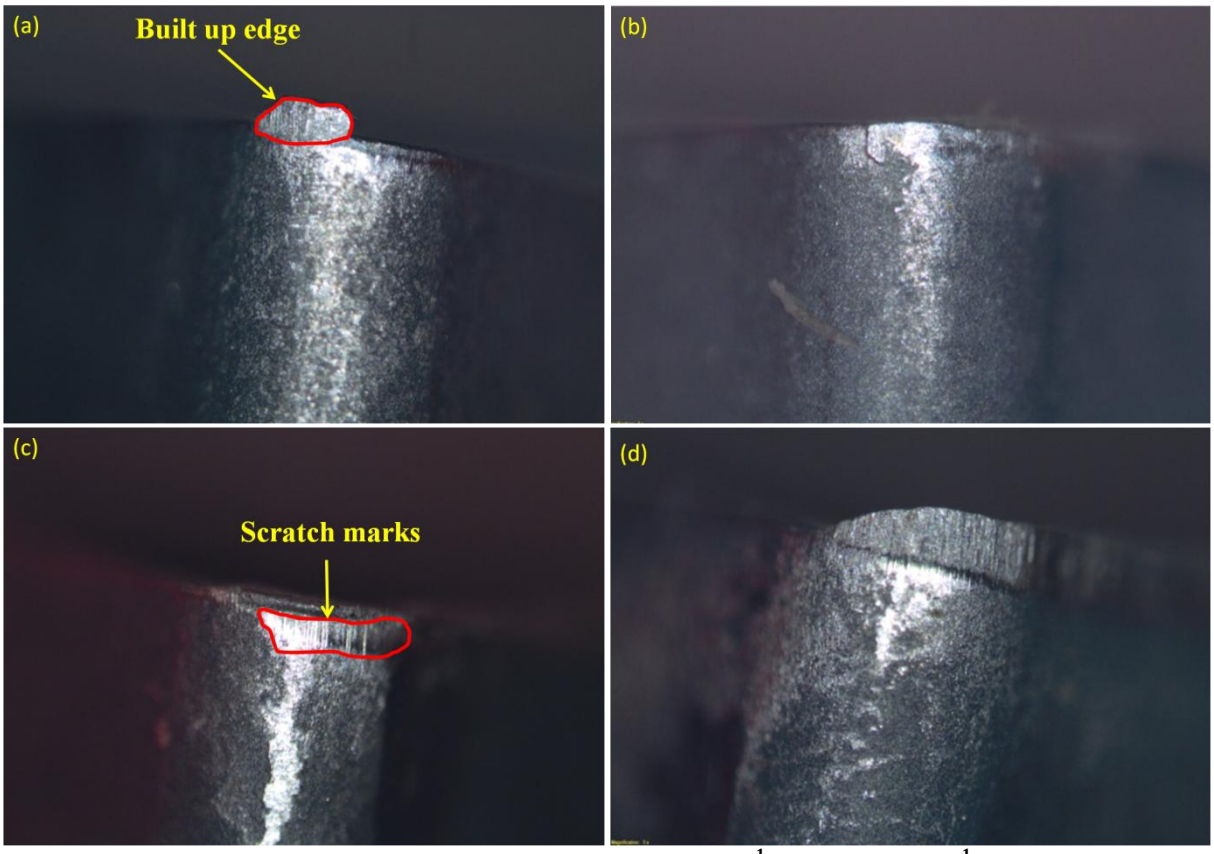

Fig. 9. Flank wear image during turning the MMC at (a) V = 40 m.min^{-1}, f = 0.04 mm.rev^{-1}, d = 0.1 mm; (b) V = 81 m.min^{-1}, f = 0.04 mm.rev^{-1}, d = 0.3 mm; (c) V = 98 m.min^{-1}, f = 0.16 mm.rev^{-1}, d = 0.3 mm; and (d) V = 154 m.min^{-1}, f = 0.16 mm.rev^{-1}, d = 0.1 mm.

B. Chip forms

Chips were collected after each turning trial of the MMC and image of some of them are presented in Fig. 10 (a-f) as illustrative. Short, C-shaped and saw-teeth shaped broken chips (Fig. 10 a) were removed at the lower level of parametric conditions. Visual inspection reveals that the chips became thicker and wider (Fig. 10 b) at higher levels of *f* and *d*. While machining at the intermediate level of *V* (81 m.min^{-1}), C-shaped broken chips along with some debris (Fig. 10 c) were observed at lower levels of *f* and *d*; however, semi-continuous and close-coiled helical chips (Fig. 10 d) were formed on increasing those parameters. At the high speed turning (154 m.min^{-1}), helical open-coiled chips (Fig. 10 e) were removed at larger depth of cut (0.7 mm); whereas, C-shaped discontinuous chips (Fig. 10 f) were formed while machining at smaller cutting depth (0.1 mm). Formation of short and discontinuous chips may be attributed to reduction of ductility of the MMC due to SiC_p addition and formation of unstable BUE on the tool tip that acted as chip breaker. High stress concentration near the reinforced ceramics, reduction of chip deformation coefficients, increase in angle of shear [21] and severe plastic deformation at the shear zone [22-23] may be the causes of broken and semi-continuous chip formation during turning the MMC.

C. Grey relational analysis

Multi-criteria decision making methods are adopted when a decision is to be taken out of various conflicting criteria [24]; however, these are troublesome to use in machining area [25]. GRA can be successfully applied for prediction and decision making in a system with less or incomplete information [26-30]. Machining is one of such system, where this method can be applied to optimize its different variables for several quality targets simultaneously [31-32]. In the present work, GRA and Taguchi method are used for simultaneous optimization of response (*Ra*, *T*, *VBc* and *M*) while cutting aluminium 7075/SiC_p composite in dry condition. Among the responses *Ra*, *T* and *VBc* are based upon "smaller is better", whereas *M* is based upon "larger is better" criteria. Results of *Ra*, *T* and *VBc* are normalized utilizing Eq. (2) and the results of *M* are normalized through Eq. (3). Coefficients of deviation are then determined using Eq. (4). Table IV presents the normalized data and deviation coefficients for all the responses. Eqs. (5) and (6) were utilized to calculate the grey relational coefficients (GRCs) of each response and grey relational grades (GRGs) of all responses [33], respectively, which are presented in Table V. The GRGs are then arranged in descending order. GRG is a quality criterion for the multiple responses under simultaneous consideration. Largest value of GRG indicates a strongest co-relation among the sequence of reference and the compatibility sequence [34]. Means of GRGs at different parametric levels are calculated and listed in Table VI. Fig. 11 portrays the main effects plot for the means of GRG. As observed from Table VI and Fig. 11, GRGs are highest for V= 154 m.min^{-1} (4th level), f = 0.04 mm.rev^{-1} (1st level) and d = 0.1 mm (1st level), i.e. for the parametric combination of V_4-f_1-d_1, which is the optimized factor setting for *Ra*, *T*, *VBc* and *M*, considering at a time.

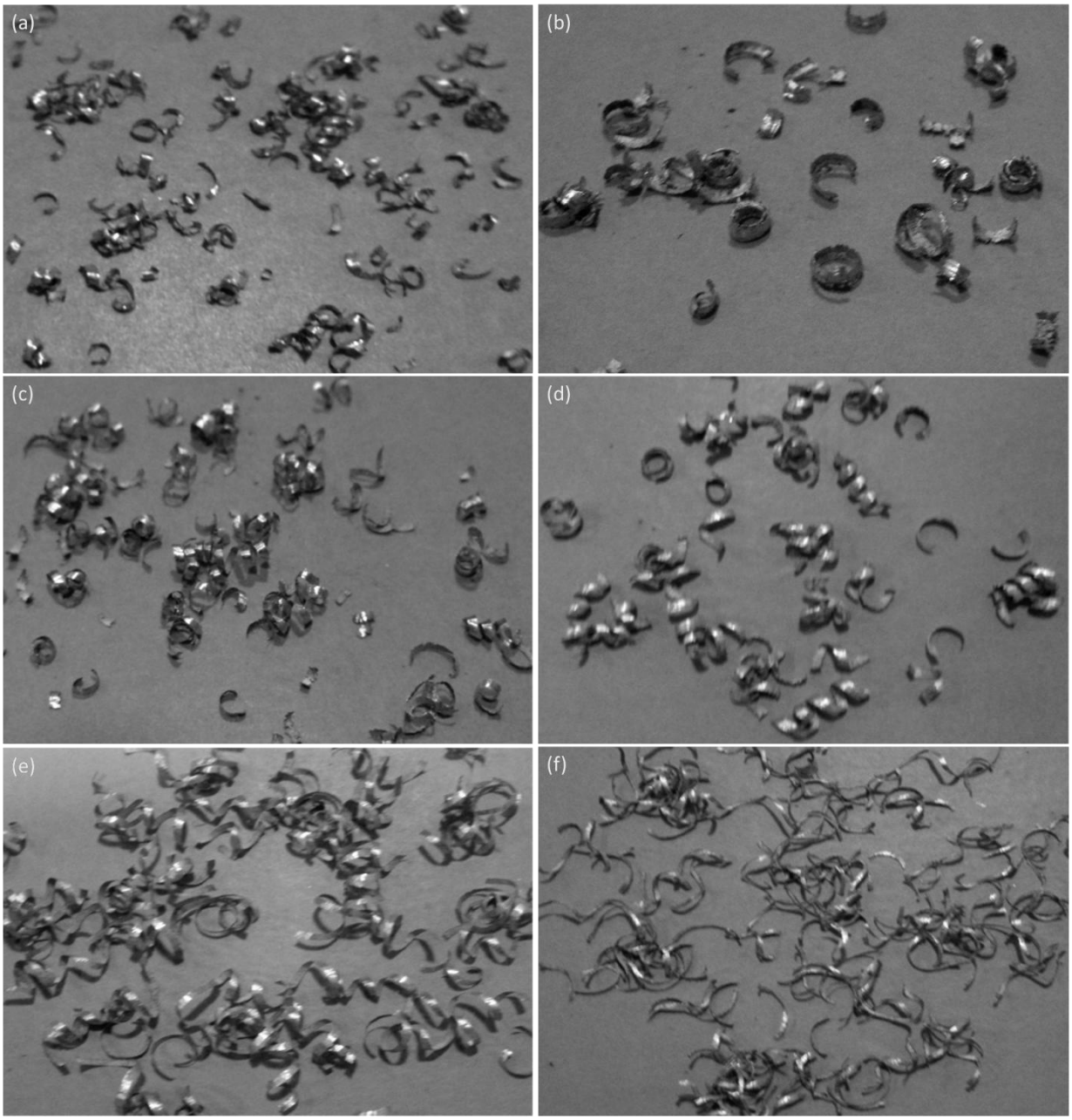

Fig. 10. Image of collected chips during turning the MMC at (a) V = 40 m.min^{-1}, f = 0.04 mm.rev^{-1}, d = 0.1 mm; (b) V = 40 m.min^{-1}, f = 0.16 mm.rev^{-1}, d = 0.7 mm; (c) V = 81 m.min^{-1}, f = 0.04 mm.rev^{-1}, d = 0.3 mm; (d) V = 81 m.min^{-1}, f = 0.16 mm.rev^{-1}, d = 0.5 mm; (e) V = 154 m.min^{-1}, f = 0.04 mm.rev^{-1}, d = 0.7 mm; and (f) V = 154 m.min^{-1}, f = 0.16 mm.rev^{-1}, d = 0.1 mm.

$$y_i^*(a) = \frac{\max y_i^o(a) - y_i^o(a)}{\max y_i^o(a) - \min y_i^o(a)} \quad (2)$$

$$y_i^*(a) = \frac{y_i^o(a) - \min y_i^o(a)}{\max y_i^o(a) - \min y_i^o(a)} \quad (3)$$

$$\Delta_{oi}(a) = \left| y_o^*(a) - y_i^*(a) \right| \quad (4)$$

$$\lambda(y_o^*(a).y_i^*(a)) = \frac{\Delta_{\min} + \xi.\Delta_{\max}}{\Delta_{oi}(a) + \xi.\Delta_{\max}} \quad (5)$$

$$\lambda(y_o^*.y_i^*) = \frac{1}{n}\sum_{a=1}^{n} \lambda(y_o^*(a).\lambda(y_i^*(a)) \quad (6)$$

where $y_i^*(a)$ = series of normalized data, $y_i^0(a)$ = initial sequence of target value for i^{th} experiment and a^{th} response [31,35-37], $\Delta_{oi}(a)$ = deviation coefficient, $y_o^*(a)$ = ideal sequence, $\lambda(y_o^*(a).y_i^*(a))$ = GRC, ξ = distinguishing coefficient (within the range 0 to1) and $(\lambda(y_o^*.y_i^*))$ = GRG for n responses.

Table IV: Normalized data and deviation coefficients

Trial No.	Normalized Data				Deviation Coefficients			
	Ra	T	VBc	M	Ra	T	VBc	M
1	0.9452	1	1	0	0.0548	0	0	1
2	0.7352	0.6459	0.7921	0.0763	0.2648	0.3541	0.2079	0.9237
3	0.2192	0.4794	0.5644	0.2197	0.7808	0.5206	0.4356	0.7803
4	0	0.2931	0.3515	0.4406	1	0.7069	0.6485	0.5594
5	0.8676	0.6304	0.8416	0.0958	0.1324	0.3696	0.1584	0.9042
6	0.6849	0.7627	0.6584	0.0598	0.3151	0.2373	0.3416	0.9402
7	0.4840	0.0836	0.4950	0.7898	0.5160	0.9164	0.5050	0.2102
8	0.3744	0.0814	0.2921	0.7791	0.6256	0.9186	0.7079	0.2209
9	0.9817	0.3693	0.7624	0.5830	0.0183	0.6307	0.2376	0.4170
10	0.7352	0.0931	0.5644	0.7536	0.2648	0.9069	0.4356	0.2464
11	0.7215	0.5076	0.3317	0.1533	0.2785	0.4924	0.6683	0.8467
12	0.4977	0.2481	0.1287	0.6653	0.5023	0.7519	0.8713	0.3347
13	1	0	0.6733	0.6743	0	1	0.3267	0.3257
14	0.8950	0.1217	0.4901	1	0.1050	0.8783	0.5099	0
15	0.6530	0.3775	0.2376	0.9167	0.3470	0.6225	0.7624	0.0833
16	0.6073	0.4631	0	0.4031	0.3927	0.5369	1	0.5969

Table V: GRCs (at $\xi = 0.5$), GRGs and their order

Trial No.	GRCs				GRGs	Order
	Ra	T	VBc	M		
1	0.9012	1	1	0.3333	0.8686	1
2	0.6537	0.5854	0.7063	0.3512	0.5742	6
3	0.3904	0.4899	0.5344	0.3905	0.4513	15
4	0.3333	0.4143	0.4353	0.4720	0.4137	16
5	0.7906	0.5750	0.7594	0.3561	0.6203	5
6	0.6134	0.6782	0.5941	0.3472	0.5582	8
7	0.4921	0.3530	0.4975	0.7040	0.5117	10
8	0.4442	0.3525	0.4139	0.6935	0.4760	12
9	0.9648	0.4422	0.6779	0.5453	0.6575	3
10	0.6537	0.3554	0.5344	0.6699	0.5533	9
11	0.6422	0.5038	0.4280	0.3713	0.4863	11
12	0.4989	0.3994	0.3646	0.5990	0.4655	13
13	1	0.3333	0.6048	0.6055	0.6359	4
14	0.8264	0.3628	0.4951	1	0.6711	2
15	0.5903	0.4454	0.3961	0.8572	0.5722	7
16	0.5601	0.4822	0.3333	0.4558	0.4579	14

Table VI: Response table for means of GRG

Level	V	f	d
1	0.5620	0.6806	0.5778
2	0.5416	0.5892	0.5580
3	0.5407	0.5054	0.5640
4	0.5843	0.4533	0.5287
Delta	0.0436	0.2273	0.0491
Rank	3	1	2

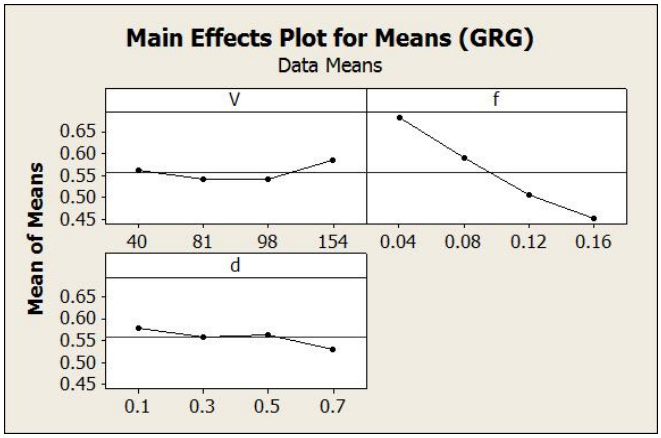

Fig. 11. Main effects plot for means of GRG.

D. Confirmation tests

Confirmation tests were carried out to verify the performance of optimized parameters and to compare with the predicted results. Second levels of all parameters were assumed as initial parametric setting during the tests. Table VII presents the results of confirmation tests, which shows a good agreement between the experimental and predicted results. Furthermore, there was an improvement of 0.1082 or 20.27% of GRG for the optimal parameters than the initial.

E. Analysis of Variance (ANOVA)

ANOVA was computed at the level of 95% confidence through MINITAB 2017 software to observe the importance of machining parameters on GRG. Outcomes of ANOVA for GRG are manifested in Table VIII. From the results, it can be concluded that only feed was significant for GRG, as it's P-value (probability of significance) was below 5%. Moreover, the tabulated F-value (Fisher's constant) at a confidence level of 95% is 4.76 [38], which is sufficiently lesser than its statistical value, i.e. 7.54. Also feed posses the highest % of contribution (74%) among all the considered parameters.

F. Mathematical models for responses

Second order mathematical models are generated using response surface methodology (RSM) for prediction of *Ra*, *T*, *VBc* and *M*. Experimental data of Table III were computed and processed by MINITAB software to develop the models. The models are demonstrated in Eqs. (7)-(10) for *Ra*, *T*, *VBc* and *M* respectively, during turning the MMC with uncoated carbide inserts. The R^2 (determination coefficient) values are 96.39%, 98.89%, 99.25% and 96.2% for *Ra*, *T*, *VBc* and *M* respectively, which are close to 100%. These are also in logical accordance with their corresponding values of adjusted R^2. Therefore, the models are adequate and fit to the data sample [39]. In the normal probability plots (Fig. 12 a-d), residuals are situated reasonably close to the lines of normal probability and distributed normally. Therefore, the models can be considered as significant as well as adequate [40].

Table VII: Confirmation test results

	Initial parameters	Optimal parameters	
		Prediction	Experiment
Level	*V2-f2-d2*	*V4-f1-d1*	*V4-f1-d1*
Ra	1.82	0.8625	0.88
T	64.43	54.4488	55.23
VBc	0.182	0.1728	0.176
M	2470.33	1831.99	1846.82
GRG	0.5336	0.7284	0.6418
Improvement in GRG =0.1082 (or 20.27%)			

Table VIII: ANOVA results of GRG

Process parameters	Degree of freedom	Sum of squares	Mean square	F	P	% of contribution
V	3	0.0051	0.0017	0.32	0.809	3.2
f	3	0.1189	0.0396	7.54	0.019	74
d	3	0.0051	0.0017	0.33	0.807	3.2
Error	6	0.0316	0.0053			19.6
Total	15	0.1607				100

$$Ra = 0.6842 + 0.0022V + 15.3629\,f + 1.0894d - 12.5\,f^2 + 0.1563d^2 - 0.0784V * f - 0.0177V * d + 6.3481\,f * d \quad (7)$$

$$R^2 = 96.39\%, R^2(adj) = 90.99\%$$

$$T = 18.315 + 0.262V + 201.049\,f + 39.617d - 0.001V^2 - 24.609\,f^2 - 17.672d^2 - 0.069V * f + 0.334V * d - 137.682\,f * d \quad (8)$$

$$R^2 = 98.89\%, R^2(adj) = 97.21\%$$

$$VBc = 0.00675 + 0.00112V + 1.14829\,f + 0.07196d + 0.66406\,f^2 + 0.01094d^2 - 0.00101V * f - 0.00049V * d - 0.50992\,f * d \quad (9)$$

$$R^2 = 99.25\%, R^2(adj) = 98.13\%$$

$$M = -673.6 + 12V - 22334.4\,f + 2592.7d - 0.1V^2 - 77063.3\,f^2 - 9976.1d^2 + 339.2V * f + 63.5V * d + 68059.9\,f * d \quad (10)$$

$$R^2 = 96.2\%, R^2(adj) = 90.49\%$$

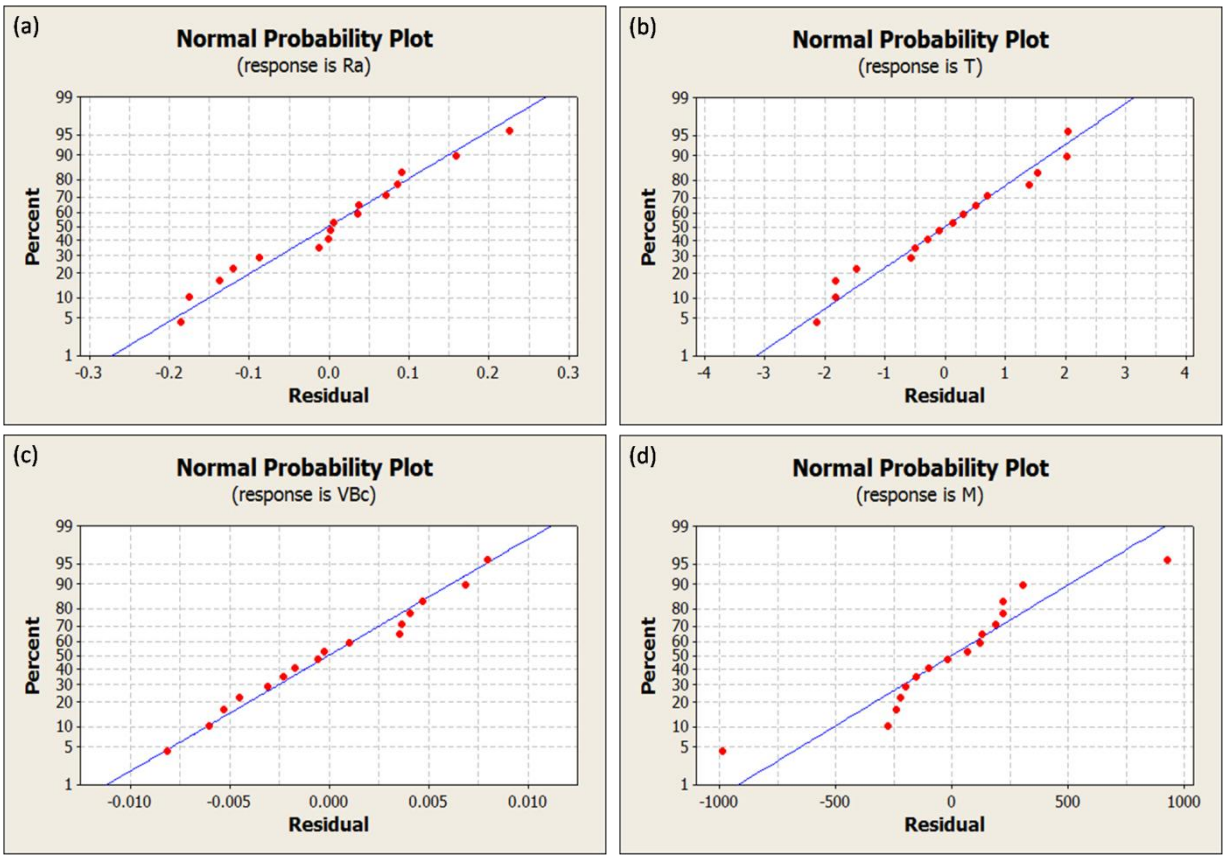

Fig. 12. Normal probability plots of residuals for (a) *Ra*; (b) *T*; (c) *VBc*; and (d) *M*.

IV. CONCLUSIONS

- Liquid metallurgy stir casting method was able to produce aluminium 7075/20 wt.% SiC_p (30.65 µm) MMC with homogeneous dispersion of the reinforcements. While turning the MMC with uncoated WC inserts in dry machining condition, minimum *Ra* (1.25 µm) was observed at *V* of 154 m.min^{-1}, *f* of 0.04 mm.rev^{-1} and *d* of 0.7 mm. There was an improvement of surface quality at higher values of *V* and lower values of *f* and *d*. Particle fracture, particle pullout and voids were observed in optical micrographs of the machined MMC surface. *T* increased on increasing any of the considered cutting factors (*V*, *f* and *d*), which was due to more heat inception at the zone of machining for increased friction. For *T*, *d* was more influential than *f*. Minimum value of *VBc* (0.101 mm) was observed at the lowest levels of machining parameters, i.e. 40 m.min^{-1}, 0.04 mm.rev^{-1} and 0.1 mm of *V*, *f* and *d*, respectively. The mean *VBc* increased with increasing either *V* or *f*; however, the influence of *d* was not significant. Principal tool wear mechanism was abrasion, though adhesion was reported at lower speed of cutting, leading to BUE formation. *M* was maximum (6105.3 mm^3/min) while turning the MMC at *V* of 154 m.min^{-1}, *f* of 0.08 mm.rev^{-1} and *d* of 0.5 mm. It enhanced on increasing the cutting parameters considered in this study.
- C-shaped and saw-toothed broken chips were produced at the lower level of parametric conditions. The chips became thicker and wider at higher values of *f* and *d*. At the intermediate level of *V* (81 m.min^{-1}), C-shaped broken chips along with some debris were observed at lower levels of *f* and *d*; however, semi-continuous and close-coil helical shaped chips were observed on increasing the *f* and *d*. At the high speed turning (154 m.min^{-1}), open-coiled helical chips were formed at larger *d* (0.7 mm); whereas, C-shaped discontinuous chips were formed while machining the MMC at comparatively smaller value of *d* (0.1 mm).

- *Ra*, *T*, *VBc* and *M* were optimized simultaneously using GRA based Taguchi method, and results revealed that the optimized parametric setting was V_4-f_1-d_1 (i.e. V=154 m.min^{-1}, f=0.04 mm.rev^{-1} and d=0.1 mm). From the confirmation tests, improvement in GRG for optimal parameters was observed to be 0.1082 or 20.27%. Results of ANOVA divulged that only feed was significant for GRG, which also possessed 74% contribution (highest among all).
- Mathematical models for *Ra*, *T*, *VBc* and *M* developed through response surface method were adequate, significant and fitted with the data sample.

ACKNOWLEDGMENT

Authors are thankful to KIIT Deemed to be University, Bhubaneswar for allowing Laboratory facility to conduct the experiments.

REFERENCES

1. S. Gopalakannan, and T. Senthilvelan, "Application of response surface method on machining of Al–SiC nano-composites", *Measurement*, vol. 46, Issue 8, 2013, pp. 2705-2715.
2. M. Ramezani, "Surface roughness prediction of particulate composites using artificial neural networks in turning operation", *Decision Science Letters*, vol. 4, 2015, pp. 419-424.
3. R.K. Bhuyan and B.C. Routara, "Optimization the machining parameters by using VIKOR and Entropy Weight method during EDM process of Al–18% SiCp Metal matrix composite", *Decision Science Letters*, vol. 5, 2016, pp. 269–282.
4. D. Das, P.C. Mishra, A.K. Chaubey and S. Singh, "Fabrication process optimization for improved mechanical properties of Al 7075/SiCp metal matrix composites", *Management Science Letters*, vol. 6, Issue 4, 2016, pp. 297-308.
5. M. Singla, D.D. Dwivedi, L. Singh and V. Chawla, "Development of aluminium based silicon carbide particulate metal matrix composite", *Journal of Minerals and Materials Characterization and Engineering*, vol. 8, Issue 6, 2009, pp. 455-467.
6. A. Kumar, M.M. Mahapatra and P.K. Jha, "Effect of machining parameters on cutting force and surface roughness of in situ Al–4.5% Cu/TiC metal matrix composites", *Measurement*, *48*, 2014, pp. 325-332.
7. Z.M. Xu, N.L. Loh and W. Zhou, "Hot isostatic pressing of cast SiCp-reinforced aluminium-based composites", *Journal of Materials Processing Technology*, vol. 67, Issue 1-3, 1997, pp. 131-136.
8. A. Manna and B. Bhattacharyya, "A study on different tooling systems during machining of Al/SiC-MMC", *Journal of Materials Processing Technology*, vol. 123, Issue 3, 2002, pp. 476-482.
9. A. Manna and B. Bhattacharayya, "A study on machinability of Al/SiC-MMC", *Journal of Materials Processing Technology*, vol. 140, Issue 1-3, 2003, pp. 711-716.
10. M. Kok, E. Kanca and O. Eyercioğlu, "Prediction of surface roughness in abrasive waterjet machining of particle reinforced MMCs using genetic expression programming", *The International Journal of Advanced Manufacturing Technology*, vol. 55, Issue 9-12, 2011, pp. 955-968.
11. A. Schubert and A. Nestler, "Enhancement of Surface Integrity in Turning of Particle74 Reinforced Aluminium Matrix Composites by Tool Design", *Procedia Engineering*, vol. 19, 2011, pp. 300-305.
12. J.T. Lin, D. Bhattacharyya and C. Lane, "Machinability of a silicon carbide reinforced aluminium metal matrix composite", *Wear*, vol. 181, 1995, pp. 883-888.
13. I. Ciftci, M. Turker and U. Seker, "Evaluation of tool wear when machining SiCp-reinforced Al-2014 alloy matrix composites. *Materials & design*, vol. 25, Issue 3, 2004, pp. 251-255.
14. X. Ding, W.Y.H. Liew and X.D. Liu, "Evaluation of machining performance of MMC with PCBN and PCD tools", *Wear*, vol. 259(7-12), 2005, pp. 1225-1234.
15. R. Venkatesh, A.M. Hariharan and N. Muthukrishnan, "Machinability studies of Al/SiC/(20p) MMC by using PCD insert (1300 grade)", *Proceedings of the World Congress on Engineering*, vol. 2, 2009, pp. 1-3).
16. H. Joardar, N.S. Das and G. Sutradhar, " An experimental study of effect of process parameters in turning of LM6/SiC P metal matrix composite and its prediction using response surface methodology", *International Journal of Engineering, Science and Technology*, vol. 3, Issue 8, 2011, pp. 132-141.
17. A.K. Sahoo, S. Pradhan and A.K. Rout, "Development and machinability assessment in turning Al/SiCp-metal matrix composite with multilayer coated carbide insert using Taguchi and statistical techniques", *Archives of civil and mechanical engineering*, vo. 13, Issue 1, 2013, pp. 27-35.
18. A.K. Sahoo and S. Pradhan, "Modeling and optimization of Al/SiCp MMC machining using Taguchi approach", *Measurement*, vol. 46, Issue 9, 2013, pp. 3064-3072.
19. P.C. Mishra, D. Das, M. Ukamanal, B.C. Routara and A.K. Sahoo, "Multi-response optimization of process parameters using Taguchi method and grey relational analysis during turning AA 7075/SiC composite in dry and spray cooling environments", *International Journal of Industrial Engineering Computations*, vo. 6, Issue 4, 2015, pp. 445-456.
20. D. Das, P.C. Mishra, S. Singh, A. Chaubey and B.C. Routara, "Machining performance of aluminium matrix composite and use of WPCA based Taguchi technique for multiple response optimization", *International Journal of Industrial Engineering Computations*, vol. 9, Issue 4, 2018, pp. 551-564.
21. Y.M. Quan, Z.H. Zhou and B.Y. Ye, "Cutting process and chip appearance of aluminum matrix composites reinforced by SiC particle", *Journal of Materials Processing Technology*, vol. 91, Issue 1-3, 1999, pp. 231-235.
22. S. Das, R. Behera, G. Majumdar, B. Oraon and G. Sutradhar, "An experimental investigation on the machinability of powder formed silicon carbide particle reinforced aluminium metal matrix composites", *Int. J. Heat Mass Transf*, vol. 50, 2011, pp. 5054-5064.
23. R. Behera and G. Sutradhar, "Machinability of LM6/SiC_p MMC with tungsten carbide cutting tool inserts", *ARPN Journal of Engineering and Applied Sciences*, vol. 7, Issue 2, 2012, pp. 216-221.
24. V.K. Koganti, N. Menikonda, S.P. Anbuudayasankar, T. Krishnaraj, R.K. Athhukuri and M.S. Vastav, "GRAHP TOP model for supplier selection in Supply Chain: A hybrid MCDM approach", *Decision Science Letters*, vol. 8, 2019, pp. 65–80.
25. H. Majumder and A. Saha, "Application of MCDM based hybrid optimization tool during turning of ASTM A588", *Decision Science Letters*, vol. 7, 2018, PP. 143–156.
26. A. Ghasemi, S. Beigilanlouei and H. Pourmahdian, "Human resource development formulation and evaluation in an Iranian Petrochemical Company using ANP and grey relational analysis", *Management Science Letters*, vol. 6, Issue 7, 2016, pp. 461-474.
27. N. Kundakci "Personnel selection with grey relational analysis", *Management Science Letters*, vol. 6, Issue 5, 2016, pp. 351-360.
28. S. Dey and S. Chakraborty, "A study on the machinability of some metal alloys using grey TOPSIS method, *Decision Science Letters*, vol. 5, 2016, pp. 31–44.
29. K. Vatansever and Y. Akgul, "Performance evaluation of websites using entropy and grey relational analysis methods: The case of airline companies", *Decision Science Letters*, vol. 7, 2018, pp. 119–130.
30. A. Zare, M.R. Feylizadeh, A. Mahmoudi and S. Liu, "Suitable computerized maintenance management system selection using grey group TOPSIS and fuzzy group VIKOR: A case study", *Decision Science Letters*, vol. 7, 2018, pp. 341–358.
31. I. Nayak, J. Rana and A. Parida, "Performance optimization in electro-discharge machining using a suitable multiresponse optimization technique", *Decision Science Letters*, vol. *6*, 2017, pp. 283–294.
32. S. Chakraborty, B. Bhattacharyya and S. Diyaley, "Applications of optimization techniques for parametric analysis of non-traditional machining processes: A Review. *Management Science Letters*, vol. 9, Issue 3, 2019, pp. 467-494.
33. S. Zarandi, V. Shahabi, M. Emami, A. Rezaee and M. Hassanloo, "Ranking banks using K-Means and Grey relational method", *Management Science Letters*, vol. 4, Issue 10, 2014, pp. 2319-2324.
34. C.L. Lin, "Use of the Taguchi method and grey relational analysis to optimize turning operations with multiple performance characteristics", *Materials and manufacturing processes*, vol. 19, Issue 2, 2004, pp. 209-220.

35. C.J. Tzeng, Y.H. Lin, Y.K. Yang and M.C. Jeng, "Optimization of turning operations with multiple performance characteristics using the Taguchi method and Grey relational analysis", *Journal of materials processing technology*, vol. 209, Issue 6, 2009, pp. 2753-2759.
36. J.H. Dahooie, A.S. Vanaki, N. Mohammadi and H.R. Firoozfar, "Selection of optimal variant route based on dynamic fuzzy GRA", *Decision Science Letters*, vol. 7, 2018, pp. 523–534.
37. P. Kumar, Meenu and V Kumar, "Optimization of process parameters for WEDM of Inconel 825 using grey relational analysis", *Decision Science Letters*, vol. 7, 2018, pp. 405–416.
38. R. Panneerselvam, "Research methodology", *PHI Learning private limited*, Second edition, 2014.
39. N.S.K. Reddy and P.V. Rao, "Selection of an optimal parametric combination for achieving a better surface finish in dry milling using genetic algorithms. *The International Journal of Advanced Manufacturing Technology*, vol. 28, Issue 5-6, 2006, pp. 463-473.
40. S. Suresha and B.K. Sridhara, "Friction characteristics of aluminium silicon carbide graphite hybrid composites", *Materials & Design*, vol. 34, 2012, pp. 576-583.

AUTHORS PROFILE

Dr. Diptikanta Das serves as Associate Professor in SME, KIIT DU, Bhubaneswar, India. He has 20 years of experience in teaching various Mechanical Engineering subjects. He has supervised eight theses in Post graduate level and one more is continuing. Three scholars are pursuing Ph.D. under his supervision. He has published 35 technical articles in various reputed journals and delivered many technical talks in various Int. conferences. He has life membership in ISTE (Indian Society For Technical Education) and ISCA (Indian Science Congress Association). His areas of research include composite fabrication and characterization, machining of composites and hard materials, tribology, multi-criteria decision-making, optimization and simulation.

Dr. Bharat Chandra Routara serves as Sr. Professor in SME, KIIT DU, Bhubaneswar, India. He was awarded with Ph.D. from JU, Kolkata in 2008. 04 numbers of scholars have completed their doctoral degree under his guidance, and 03 are continuing currently. He has publications in various journals indexed in SCOPUS and SCI. He has life membership in ISTE (Indian Society For Technical Education) and ISCA (Indian Science Congress Association). His areas of research include composite materials, surface morphology, micro machining, cryogenic machining, multi-criteria decision-making and optimization.

Dr. Basanta Kumar Nanda serves as Associate Professor in SME, KIIT DU, Bhubaneswar, India, and have teaching experience of 25 years. He was awarded with Ph.D. from VSSUT, Odisha in 2019. 01 scholar is continuing doctoral research under his guidance. He has publications in various journals indexed in SCOPUS and SCI. His areas of research include composite materials, surface morphology, micro machining, cryogenic machining, multi-criteria decision-making and optimization. He has life membership in ISTE (Indian Society For Technical Education) and ISCA (Indian Science Congress Association). Interests of research include nonconventional machining, surface morphology, multi-criteria decision-making and optimization.

Mr Soham Chakraborty was a student of SME, KIIT DU, Bhubaneswar, India. He was awarded with B. Tech. degree in the year 2015. His areas of research include composite fabrication and characterization, machining of composites and hard materials, tribology, multi-criteria decision-making, optimization and simulation.